Available online at www.sciencedirect.com
ScienceDirect
Journal of Power Sources 182 (2008) 429–440
JOURNAL OF POWER SOURCES
www.elsevier.com/locate/jpowsour

Analysis of a PEMFC durability test under low humidity conditions and stack behaviour modelling using experimental design techniques

Bouchra Wahdame [a], Denis Candusso [b,*], Fabien Harel [b], Xavier François [a], Marie-Cécile Péra [a], Daniel Hissel [a], Jean-Marie Kauffmann [a]

[a] *Laboratory of Electrical Engineering and Systems (L2ES, UFC–UTBM, EA 3898), FCLAB, rue Thierry Mieg, bät. F, 90010 Belfort Cedex, France*
[b] *The French National Institute for Transport and Safety Research (INRETS), FCLAB, rue Thierry Mieg, bät. F, 90010 Belfort Cedex, France*

Received 30 October 2007; received in revised form 19 December 2007; accepted 31 December 2007
Available online 17 January 2008

Abstract

A polymer electrolyte membrane fuel cell (PEMFC) stack has been operated under low humidity conditions during 1000 h. The fuel cell characterisation is based both on polarisation curves and electrochemical impedance spectra recorded for various stoichiometry rates, performed regularly throughout the ageing process. Some design of experiment (DoE) techniques, and in particular the response surface methodology (RSM), are employed to analyse the results of the ageing test and to propose some numerical/statistical laws for the modelling of the stack performance degradation. These mathematical relations are used to optimise the fuel cell operating conditions versus ageing time and to get a deeper understanding of the ageing mechanisms. The test results are compared with those obtained from another stack operated in stationary regime at roughly nominal conditions during 1000 h (reference test). The final objective is to ensure for the next fuel cell systems proper operating conditions leading to extended lifetimes.

Keywords: PEMFC; Durability; Reliability; Low humidity conditions; Experimental design; Electrochemical impedance spectroscopy

1. Introduction

The durability and the reliability criteria are of major concerns for the development of the polymer electrolyte membrane fuel cell (PEMFC) [1–6]. Furthermore, the lifetime targets (for example, 5000 h at least for car applications) must be reached while the prices of the FC systems must be decreased simultaneously. One way to achieve cost-effectiveness is to minimise the number, the complexity and the size of the FC ancillaries. Thus, one possible research way is to evaluate some solutions allowing the reduction of the external gas humidification section. Indeed, excessive gas hydration is obviously accompanied by additional energy losses (especially due to the heating of the humidifier) and it makes the water balance difficult in the particular case of embedded FC generators. The amount of water to carry in the vehicle for humidification purpose has to be limited in these autonomous systems and the water produced by the chemical reaction should be utilised as much as possible. A too high gas humidification is also a possible source of non-homogeneousity in the reactive gas and current distribution inside the stack. A flooding event is generally sudden and therefore very difficult to control. Furthermore, some flooding of the electrode regions, inducing some local starvation phenomena, can affect the FC lifetime. Nevertheless, it is also largely observed that low-humidified gas conditions lead to worse performances of FC stacks equipped with conventional perfluorinated ionomer (such as Nafion^{TM}) membranes. Indeed, proper hydration of these membranes is critical to maintain their conductivity [7]. The voltage decay due to the change of the membrane resistances can generally be restored if sufficient membrane

* Corresponding author. Tel.: +33 3 84 58 36 33; fax: +33 3 84 58 36 36.
E-mail addresses: bouchra.wahdame@utbm.fr (B. Wahdame), denis.candusso@inrets.fr (D. Candusso), fabien.harel@inrets.fr (F. Harel), xavier.francois@utbm.fr (X. François), marie-cecile.pera@univ-fcomte.fr (M.-C. Péra), daniel.hissel@univ-fcomte.fr (D. Hissel), jean-marie.kauffmann@univ-fcomte.fr (J.-M. Kauffmann).

0378-7753/$ – see front matter © 2008 Elsevier B.V. All rights reserved.
doi:10.1016/j.jpowsour.2007.12.122

water content is obtained again after a dehydration phase. The FC degradation and the irreversible loss of performance due to a decrease of the membrane mechanical stability shall be considered as well. It is admitted that low humidity condition is one of the severe environment constraints, which can have strong impacts on the lifetime and reliability of FC systems.

Many PEMFC are tested and operated under highly humidified conditions (relative humidity close to 90% in the stack) in order that the membranes remain well hydrated. However, different experimental and theoretical studies have already been devoted to various aspects of PEMFC behaviour under low-humidified conditions. In [8], Yoshioka et al. have determined the effect of low-humidified conditions on current distribution in a practical operating cell by using a segmented FC. Then, they have also conducted an endurance test over 5000 h on a 20-cell stack fed by air (relative humidity of 74% with stack temperature of 75 °C) and by a reformat mix (relative humidity of 57%). Büchi and Srinivasan have also shown in [9] that stable FC performances could be possibly obtained without humidifying the gas streams through the use of the water produced by the reaction. In [10], the effects of a reactive gas systematic dehydration on a FC performance are described by Atkins et al. Besides, a specific design of a stack flow-field is proposed in [11] by Qi and Kaufman with the aim to allow the FC operation under dry reactant conditions. Thanks to a double-path-type counter-current flow-field design, the water produced by the FC can hydrate dry reactants.

The L2ES laboratory based on the FC test platform of Belfort currently carries out research on small 100 W PEMFC stacks. This work is done with the final objective to ensure for the FC systems proper operating conditions, leading to high power and efficiency delivery, and to high performances as well in terms of reliability and durability. As L2ES and INRETS work together on FC by focusing on the system aspect, one important goal is to evaluate and to adapt the technological choices made for the various needed FC ancillaries (e.g. humidification units) in order to increase stack lifetime. A first experiment was devoted to the test of a 100 W three-cell stack operated in stationary regime at roughly nominal conditions during 1000 h [12]. This first experiment serves as reference test for the other studies that are led on other 100 W stacks and in different environment conditions. In a second stage, another 100 W stack was placed during about 700 h under dynamical current constraint linked to vehicle road cycle [13]. The third experiment, which is the object of the proposed paper, consists in an ageing test performed during 1000 h with a PEMFC fed by dry hydrogen and low-humidified air. The goal is to investigate the stack behaviour, its failure modes, the degradation causes and mechanisms related with low humidity conditions. Obviously, as the FC durability experiments are expensive and time consuming, the tests have also to be carefully implemented and exploited. Therefore, well-suited methodologies have to be adopted as well as efficient and practical tools for the test analyses. Some techniques derived from the response surface methodology (RSM) are developed with this aim in view [14,15].

The paper is organized as follows. In the next part, the experimental set-up and the conditions of the durability tests performed in the first case at nominal stack temperature and in the other case at higher temperature are described. In the third section, some results obtained from the FC characterisation procedures (polarisation curves and electrochemical impedance spectroscopy (EIS) measurements) are presented and some physical explanations are given about the results obtained. In the fourth part, a brief description concerning the design of experiment (DoE) methodology is provided. Then, some models are proposed in order to analyse the experimental results collected thanks to various RSM tools. Some optimisations are performed to select the most appropriate conditions leading to the highest voltage efficiencies.

2. Experimental set-up and test procedures

2.1. Experimental set-up

The PEMFC stacks used in this study have been assembled with commercial membranes (Gore MESGA Primea Series 5510; active cell area of 100 cm^2), gas diffusion layers and machined graphite flow distribution plates. The FC operates at atmospheric pressure (maximal pressure of 1.5 bar abs.) and their temperatures are controlled using a deionised water circuit. A detailed description of the 1 kW test bench used for the durability tests can be found elsewhere [16,17]. Many physical factors involved in the stack can be controlled and measured in order to master the FC operating conditions as accurately as possible. For instance: stack temperature, gas flows, fluid hygrometry rates, air dew point temperature can be imposed by the process. In order to achieve the air hydration, the cathode reactant is passed through a bubbler humidifier before entering the FC stack [18]. Inlet and outlet flows, pressures, temperatures, single cell voltages, and load current can be monitored thanks to a homemade interface developed with Labview™.

2.2. Test conditions

2.2.1. For the reference ageing test

The first experiment was devoted to the operation of a FC during 1000 h in stationary regime, approximately at nominal conditions. Indeed, the FC had to deliver a 50 A current (current density of 0.5 A cm^{-2}). The FC temperature was regulated at 55 °C (considering the stack outlet temperature of the cooling loop). The FC was fed by dry hydrogen and humidified air. The set of anode/cathode stoichiometry rates (FSA/FSC) was fixed to 2/4, respectively. The FC was operated in open mode: the air and hydrogen flows were controlled by flow regulators placed upstream of the stack. The air dew point temperature was 25 °C, which corresponds to a relative humidity close to 22% inside the stack (value computed not taking into account the production of water through the chemical reaction). This value was set regarding the manufacturer recommendations. Nevertheless, it can be noticed that this relative humidity rate is already low in comparison with the values usually adopted for PEMFC equipped with perfluorosulfonic acid membranes [8,19].

2.2.2. For the ageing test performed at low humidity conditions

Another durability experiment has consisted in operating another FC under low humidity conditions and with a time target of 1000 h. As in the case of the first ageing experiment, the load current was regulated at 50 A. The FC was also fed by dry hydrogen and humidified air (air dew point temperature of 25 °C) using a FSA/FSC set equal to 2/4. Unlike the first ageing test, the FC temperature was controlled at 65 °C, which corresponds to a temperature level 10 °C higher than the reference one and to a relative humidity rate in the stack of 15% at air side. Many parameters (load current, stack voltage, temperatures, gas flows, pressures, etc.) were recorded continuously over the 1000 h test duration. Nevertheless, simply acquiring these data on the stack throughout the durability test will not be sufficient to get a comprehensive understanding of the degradation mechanisms. The FC must also be well characterised during the ageing experiment. The additional collected data will help us to determine and quantify the degradation that occurs over long periods. Thus, for the investigated FC stacks, two types of characterisation (polarisation curve test and stack impedance measurement) were performed at regular time intervals—twice in a week. The durability test was stopped just before each characterisation sequence (total duration approximately equal to 6 h), and restarted after the completion of this sequence. Notice that the characterisation hours are included in the duration total accounts. Moreover, several initial characterisation sequences have been achieved before the beginning of the durability tests, in particular to check the repeatability of the measurements.

Before any polarisation test, it is usually recommended to operate the FC in steady-state conditions in order to avoid as far as possible any impact of the recent chronological account on the characterisation measurement [20,21]. In the low humidity test, the adopted conditioning procedure has consisted in operating the FC always in the same conditions at 50 A (FSA/FSC set equal to 2/4, temperature of 55 °C) during 30 min, prior to each characterisation sequence. During each characterisation, five different polarisation curves were consecutively recorded, for FSA/FSC sets equal to 2/5, 2/4, 2/3, 1.5/3.5 and finally 1.5/4. Notice that only four FSA/FSC sets were considered in the first reference test: 2/5, 2/4, 2/3 and 1.5/3.5. A polarisation record was realised by incrementing the FC current from 0 to 70 A (current density of 0.7 A cm^{-2}) by steps of 0.5 A. Once the polarisation curves were recorded, impedancemetry technique was used to investigate the dynamical stack behaviour.

The EIS measurements were performed with a Zahner-Kronach, Germany-impedancemeter (IM6 and PP240 devices). The study of the dynamical FC behaviours was carried out in galvanostatic mode, considering a static operation point (polarisation current of 35 A) and a small sinusoidal alternating part (amplitude of 1 A). Each impedance spectrum is a series of single impedance measurements at discrete frequency points. The data density and the measurement accuracy were selected considering the steps per frequency decade and the number of measured periods. The frequency of sinusoidal perturbation was here ranging from 30 kHz to 10 mHz. Impedance spectra have been measured in the following steady-state conditions: FC temperature was 55 °C, the air dew point temperature was equal to 25 °C, anode/cathode stoichiometry rates were equal to various FSA/FSC sets: 2/5, 2/4, 2/3, and 1.5/3.5 as well as 1.5/4 but not systematically. Notice that the dynamical behaviour of the FC that served for the reference test was investigated considering a single FSA/FSC set only: 2/5. Once the spectra were recorded, the physical parameters (stack temperature of 65 °C, stoichiometry rates, load current) related to the durability test were set again and the ageing experiment in low humidity conditions could immediately go on. Note that some additional and more detailed information about the characterisation methodologies can be found in [16,17].

3. Experimental results

3.1. Evolution of physical quantities over test duration

3.1.1. For the reference ageing test

Fig. 1 shows the stack voltage that was recorded continuously. The variable is plotted each 24 h, but not during the characterisation sequences. Except at the very beginning of the test (where a slight improvement of the voltage could possibly be detected), the stack exhibits quite constant voltage during the first 350 h of the experiment. Then degradation has occurred quite rapidly during the following 50 h (with a rate of about 300 mV/100 h for the stack). Finally, a quite low steady degradation rate (about 20 mV/100 h) can be observed until the end of the test. If the voltage evolution versus time has to be modelled by a single mathematical relation, a fifth order polynomial equation can be proposed (Fig. 1). No important failure compromising the physical stack integrity has been encountered during the test.

3.1.2. For the low humidity ageing test

As already mentioned, the duration of the test was initially expected to be 1000 h but unfortunately a membrane failure was encountered around the 450th hour of stack operation. A typical pressure test performed with nitrogen at anode allowed to detect a gas leakage inside the stack. Although the hypothesis of sealing deteriorations cannot be dismissed, the most probable cause of the leakage is a break (or hole) in a membrane leading to reactive gas crossover between anode and cathode. The failed cell was detected by considering the abnormal behaviour

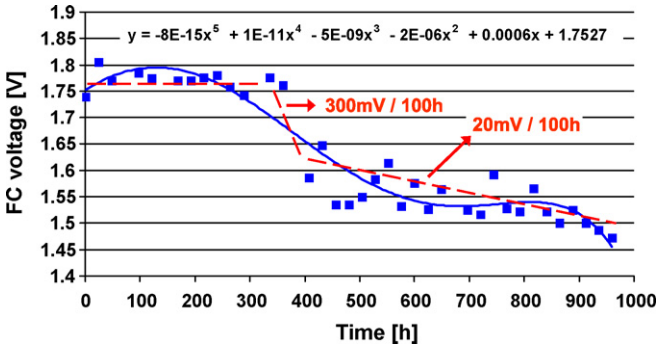

Fig. 1. FC stack voltage vs. time for the reference experiment (stack temperature of 55 °C).

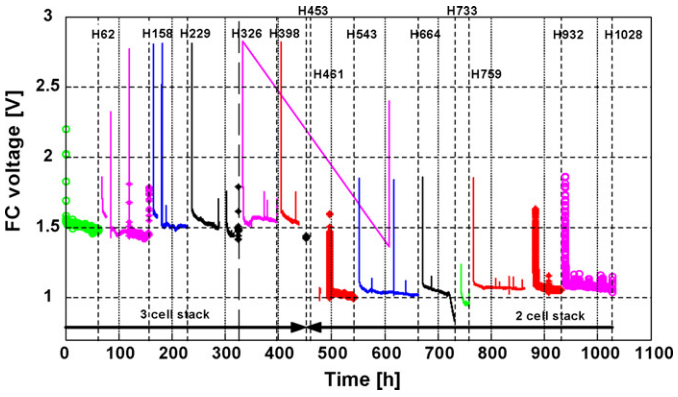

Fig. 2. FC stack voltage vs. time for the low humidity experiment (stack temperature of 65 °C).

of its open current voltage (OCV) after the shutdown of the reactive gases. Actually, a rapid drop down of the cell voltage was observed while the other safe cells could keep usual high potentials. Then, after this diagnosis procedure, the defective cell was removed. From that time, we chose to continue the experiment with the stack composed of the two remaining safe cells. Afterwards, no other problem occurred with the investigated FC until the end of the test. The stack voltage evolution, during the phases where the FC temperature and current references are equal to 50 A and 65 °C, respectively, is plotted in Fig. 2. The voltage is first displayed for the period corresponding to the stack made of three cells and then in the case of the two-cell stack. The global evolutions of the FC voltages during each one of the two time intervals show that no notable regular degradation occurred during the test. On the contrary, after each characterisation sequence, the FC voltage is subjected to a kind of reversible decrease, which is fast the first hour because of the stack temperature increase from 55 °C to 65 °C, and then both slower and slighter the following hours when the stack temperature of 65 °C is kept constant. This drop down of the FC performances observed after the characterisation sequences can be attributed to the gradual dehydration of the cells and thus to the water removal process from of different layers within the FC plates and membrane electrode assemblies (MEAs). In this way, we can also speculate on the following possible scenario. At the beginning of the new steady-state current phase, some water in the flow-field channels and at the GDL surfaces might be removed first. Then, as the drying process goes on, some water may be removed from the porous GDL and from the membranes. But further studies coupling both experiment and modelling tasks are still required to provide a detailed description of the underlying phenomena (related to water and mass transports inside the cell) causing the changes in the cell voltages with the different time constants observed. The other small peaks linked with some sudden increases of the voltage correspond most of the time to some short interruptions of the load current and stops of the pump on the cooling circuit (duration around 30 s). These pump shutdowns are caused deliberately in order to flush some air bubbles out of the deionised water loop. This is sufficient to lead to a rapid decrease of the stack temperature, down to about 55 °C, and consequently to a fast improvement of the FC electrical efficiency (recovery time of a 10 s). However, after the start-up of the cooling pump, the stack temperature reaches 65 °C again in about 1 min and the FC shows a voltage level, which is similar with the one measured just before the beginning of the flushing process. A very slight improvement of the FC performance might even be detected if the global evolution of the "mean cell" voltage over the complete test duration is considered (around 20 mV over the 1000 h). Notice that the quality of the stack temperature and reactive gas flow controls, and their constancies over the ageing time, are crucial in such a durability test. It is also very important to be sure that no gas leakage occurs upstream of the stack. Indeed, at the 65 °C temperature, a leakage on the air pipe (corresponding for instance to a change of the FSC condition from 4 to 3.5) would lead to significantly higher FC voltages. The impact of such changing conditions will be evaluated in the next sections.

3.2. Polarisation curve results

The set of the polarisation curves recorded during the reference ageing test for FSA/FSC = 2/4 is represented together using a three-dimensional (ageing time–FC current–FC voltage) shaded surface (Fig. 3). Its projection, a contour plot beneath the surface, is drawn in the time–current plane. This plot is like topological maps, which show elevation versus both longitude and latitude. However, instead of elevation, the map shows here the levels of the measured FC voltage versus two variables: time and

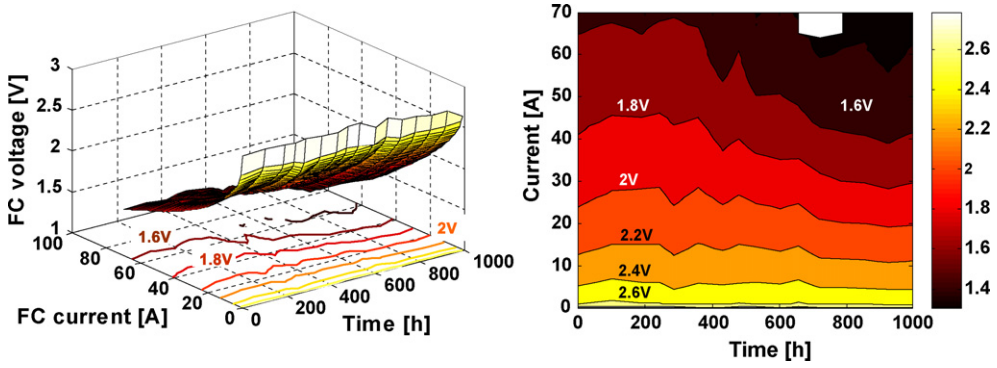

Fig. 3. Display of the polarisation curve set in the case of the reference ageing test, first using a three-dimensional shaded surface and then a two-dimensional representation (FSA/FSC = 2/4).

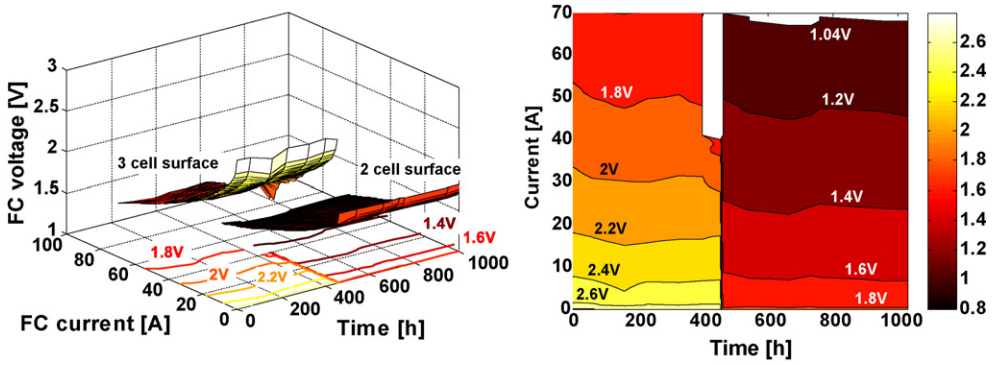

Fig. 4. Display of the polarisation curve set in the case of the test in low humidity conditions (FSA/FSC = 2/4).

load current. Obviously, the same kind of representation can also be used for the other stoichiometry sets and for the ageing test performed in low humidity conditions. So defined, the contour plot can be displayed in a two-dimensional way (time–current plane), which may let the FC voltage degradations more clearly appear and make the analyses easier. The same representative approach can obviously be adopted for the test performed with a stack temperature of 65 °C (Fig. 4). Because of the cell failure observed during the test, it leads to two different surfaces if the stack voltage is considered. In Section 4, a single surface will be drawn by considering a "mean single cell" voltage, which is basically computed from the total stack voltage and the number of cells.

In addition, we would like to point out the fact that an absence of voltage measurement could sometimes be detected from the records of the polarisation curves. For instance, in the case of the reference test, the curve measured at $t = 655$ h could not be recorded completely for current values up to 70 A. This was due to an intermittent potential profile inducing the crossing of a cell voltage under the minimal threshold of 380 mV for a load current close to 65 A (which may be caused by a sudden uneven flow distribution in the FC and led automatically to the interruption of the polarisation curve record). Some absences of voltage can also be detected from the surface of Fig. 4 related with the test in low humidity conditions, especially before that the cell failure occurs and for load currents higher than 40 A. In this case, the problem is most probably induced by a gradually larger crossover rate of reactive gases through the failing membrane. In this hypothesis, a perforation or leak in the membrane of the defective cell can cause the fuel and air streams to mix, chemically react or combust thereby leading to a significantly reduced cell potential.

3.3. Impedancemetry results

All the impedance spectra recorded during the two considered durability tests are plotted in Figs. 5 and 6 (for FSA/FSC = 2/5). The spectra are displayed in the complex plane. Each impedance plot is composed of several parts. For example, let us consider the impedance spectrum measured at the 'beginning of life' of the stack used in the reference test ("H0" curve). An inductive part is present at high frequencies (between 30 kHz and 4 kHz

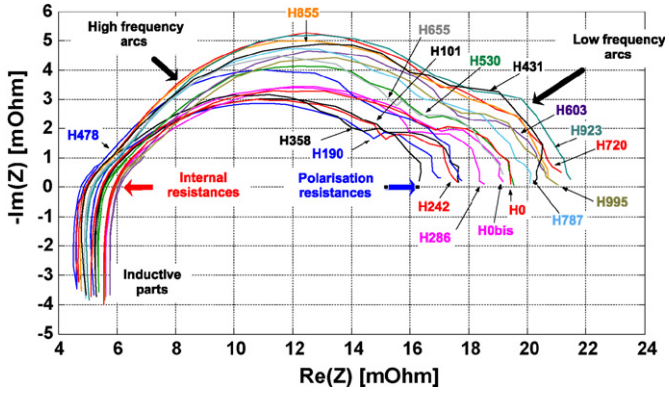

Fig. 5. Set of impedance spectra recorded during the reference durability test (for a 55 °C stack temperature).

approximately); it is due to the various FC connection elements and electric wires. A first capacitive arc (in the 4 kHz–130 Hz frequency range) and a second capacitive arc (for frequencies between 130 Hz and 0.2 Hz) appear. They correspond mainly to charge transfer phenomena (electrons and protons) at high frequencies and are related to mass and water transport at lower frequencies. The larger the arc diameters are, the more difficult are the transfer of the electrical charges and the diffusion of the reactants. We can focus on some particular locus of the impedance spectrum diagrams as the point, from which the FC internal resistance can be estimated (at high frequency, where the

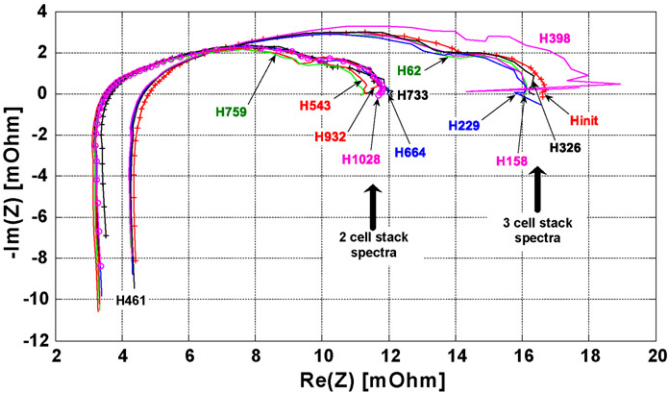

Fig. 6. Set of impedance spectra recorded during the durability test performed at 65 °C (EIS measurements performed at 55 °C like in the reference test).

imaginary part of the FC impedance equals 0). It is well known that the internal resistance strongly depends on the membrane water content. Its value is therefore related to the gas humidification process and to the amount of water carried by the humidified reactant gases. It depends also on the water quantity generated at the cathode, on the water diffusion, as well as on the electro-osmotic drag (i.e. the water molecules carried by the protons through the membrane from the anode to the cathode). Another key-point is the polarisation resistance, which can be measured at low frequencies and determined from the point on the spectrum diagram where the imaginary part of FC impedance equals 0. The in situ and non-invasively recorded impedance spectra can give some important information on the ageing of the various MEA key components. The physical interpretation of the spectra should allow understanding, up to a point, if for instance membranes and gas diffusion layers separately degrade with different ageing rates. The EIS can also be used as a diagnosis tool, which enables providing some electrical signatures linked with different possible failure modes. Notice for instance the unstable FC operation at low frequency (around 0.1 Hz) at the 398th ageing hour in the case of the test performed at 65 °C (Fig. 6). This abnormal pattern can be interpreted as a symptom of an internal gas leakage inside the stack.

4. Modelling of the fuel cell performance through ageing time

Such graphs like Figs. 3–6 are already helpful to provide quite good and simple visual representation of FC ageing. However, some techniques coming from the response surface methodology can be adopted to lead further and deeper analyses of durability experiment results. So, this approach is used to investigate the impact of ageing time over the FC stack voltage in the case of the experiment carried out in low humidity conditions. In particular, if the optimal FC operating conditions leading to the highest stack voltage versus ageing time have to be found (or possibly the operating conditions highlighting the degradation of the fuel cell performances), some various current and FSA/FSC levels have to be considered. For these purposes, some numerical/statistical models of the FC degradation are needed.

4.1. Brief overview of the DoE methodology

Actually, the design of experiment methodology dates from the beginning of the last century with the work of Fisher (1925). But in the 1960s and 1970s, many innovations were brought by Taguchi [22]. His work enabled the dissemination of the experimental designs in the business world. As a matter of fact, the purpose of the DoE method is to increase the productivity of the experimental process: especially by minimising the number of test runs when many parameters are studied and by maximising the accuracy of the results. The method allows determining the significant factors affecting the studied process and it can also highlight some possible interactions between the various factors. It is a structured, efficient procedure to plan some experiments and to obtain some data, which can be analysed in order to yield valid and objective conclusions about the studied product or process. The DoE techniques are largely used in the research of new materials or advanced component designs, even in the field of FC [23]. They are also helpful to estimate the performances of electrochemical devices like batteries [24] or capacitors [25]. In the specific research area related with FC systems, the DoE method can be used to evaluate the respective impacts of some physical control parameters (such as load current, stack temperature, gas flows, pressures, etc.) over the FC operation [26,27,7]. In these cases, the stack voltage or FC power are observed, but only during a limited time period and not to broach specific FC lifetime problems. In [28], Ordonez et al. have also used the DoE methodology, first to build up a model for a Direct Methanol FC and then to track the maximum power point.

Anyway, a large number of experimental tests are generally needed to correctly determine the performances of a FC system or to identify the parameters of a FC physical model. The choice of an experimental design depends on the objectives of the experiment and on the number of factors to be investigated [29]. The RSM is one important particular aspect of the DoE methodology. In this case, the experiment is designed to estimate the effects, the quadratic effects and the interactions of a few important factors, which have been selected before using some screening procedures. The RSM gives then an idea about the shape of the investigated response surface. The RSM designs are used to find improved or optimal process settings, troubleshoot process problems and weak points, to make a product or a process more robust. The general expression of the RSM analytical models is simple when written in a matrix form:

$$\hat{y} = X \cdot \hat{\beta} \tag{1}$$

y is the vector of the experimental results, $\hat{y}$ is the vector of the polynomial approximation at each experimental point ($y = \hat{y} + \varepsilon$ with the ε variable corresponding to the fitting error). X stands for the experimental matrix, also called design matrix. It depends on the experimental point position and on the type of polynomial model used.

$\hat{\beta}$ is the estimated coefficient vector. It is calculated with Eq. (2) describing the least square estimator.

$$\hat{\beta} = (X^{t} \cdot X)^{-1} \cdot X^{t} \cdot y \tag{2}$$

The models used in the RSM methodology take usually either a linear form or a quadratic form. Eq. (3) is a possible expression for the model.

$$\hat{y} = \beta_0 + \sum_{i=1}^{k} \beta_i \cdot x_i + \sum_{i=1}^{k} \beta_{ii} \cdot x_i^2 + \sum_{i=1}^{k} \sum_{j>i}^{k} \beta_{ij} \cdot x_i \cdot x_j \tag{3}$$

Some normalised centred representations (also called sometimes "coded values") are generally adopted for the factor levels. Then, the −1 and +1 values are, respectively, related to the minimal and maximal levels of the x factors ($-1 \le x \le +1$). The interest of such a representation lies in the fact that the values of the β coefficients can be easily interpreted. Indeed, β_0 is the arithmetic mean value of the responses, β_i are the factor effects, β_{ii} are the quadratic effects, and β_{ij} are the interactions between factors.

Once a suitable approximation for the true functional relationship between the independent variables and the surface

response is found, the optimisation of the response variable y can be made.

4.2. Static current–voltage characteristics

The static test results of the durability experiment performed at 65 °C are employed to investigate the impact of ageing time over the FC voltage, by considering some various load current and FSC levels. For this purpose, one RSM full factorial design is firstly used to analyse the endurance test and to establish a preliminary model for the FC voltage degradation. The regression model is then used to find the optimal operating conditions versus ageing time leading to the highest stack voltages.

4.2.1. Use of a full factorial design for the data selection

A full factorial design allows measuring the responses of every possible combination of factors and factor levels. These responses are generally analysed to provide some information about every main effect and every interaction effect. A full factorial DoE is practical when less than five factors are investigated. Moreover, with this type of design, orthogonality criterions are satisfied [29]. The number of needed experimental responses depends on the numbers of factors and levels adopted for each factor. However, taking into account the data recorded, a stricto sensu full factorial design cannot be used here. Indeed, as mentioned in Section 2.2, the stack performances were not investigated for FSA/FSC equal to 1.5/3. Instead of that, a non-conventional design with the ragged point FSA/FSC = 1.5/3.5, close to the missing one, is adopted. In our study, the experimental design factors considered are the ageing time (t), the hydrogen and air stoichiometry rates (FSA and FSC) and the load current (I). The output voltage of the "mean cell" ($U_{\text{mean cell RSM}}$) is the response. The levels adopted for the factors are summarised in Table 1.

Table 1
Levels of the investigated factors

Factors	Levels			
	Minimum (−1)	Intermediate	Maximum (+1)	Number
I	0 A	Step of 1A	70 A	71
t	0 h	Characterisation instants	1028 h	13
FSC	3		4	2
FSA	1.5		2	2

4.2.2. Modelling and representation by contour plots

The quadratic model generated by the design is given by (4). Some normalised centred representations are adopted for the factor levels. The regression used for the estimation of the polynomial parameters is made thanks to the *rstool* function of Matlab™ [30]. This function performs the interactive fit and plot of a multidimensional response surface.

$$\begin{aligned} U_{\text{mean cell RSM}} &= 0.633 - 0.174 \times I - 0.006 \times t + 0.001 \times \text{FSC} + 0.006 \times \text{FSA} \\ &+ 0.063 \times I^2 - 0.001 \times t^2 + 0 \times \text{FSC}^2 + 0 \times \text{FSA}^2 - 0.007 \times I \times t \\ &+ 0.005 \times I \times \text{FSC} + 0.010 \times I \times \text{FSA} + 0.004 \times t \times \text{FSC} \\ &- 0.001 \times t \times \text{FSA} + 0.003 \times \text{FSC} \times \text{FSA} + \varepsilon \end{aligned} \quad (4)$$

The model and its β values show the importance of the current impact over the stack voltage in comparison with the influences of ageing time, FSA and FSC factors. The model highlights also each relative importance of the various interactions: $I \times \text{FSA}$ and $I \times t$ are the largest ones.

One advantage of using a low order polynomial is that the response is effectively smoothed. This is essential if the main aim is to get a satisfying overall picture of the response variation. The choice concerning the model order and the interactions to be taken into account in the model has an influence on the descriptive quality of the model. A measure of the fit goodness is the norm of the residual vector: the smaller the norm is, the better the fitting is. Examining the R^2 coefficient of the multiple regression correlation is another key part of all statistical modelling. This coefficient is a number between 0 and 1. A value close to 0 suggests a poor model. If the R^2 is equal to 1, it means that the model exactly fits the measurements and totally explains the studied phenomena. The R^2 coefficient is defined by the following equation:

$$R^2 = \frac{\hat{y}^{\text{t}} \cdot \hat{y} - \bar{y}^{\text{t}} \cdot \bar{y}}{y^{\text{t}} \cdot y - \bar{y}^{\text{t}} \cdot \bar{y}} \quad (5)$$

where $\bar{y}^{\text{t}} \cdot \bar{y}$ is the sum of the squares for the mean response vector.

The R^2 coefficient, equal to 0.9812, reveals the accuracy of the chosen model. The relationship between the investigated variables was further elucidated using the predicted model (1) together with contour plots (Fig. 7). The most influential factor over the "mean cell" voltage is obviously the load current. A large performance loss is noticed at higher current densities, owing to mass-transport loss characteristics in the MEA. The lowest stoichiometry rates lead to lower voltages. The decrease of the performances versus time is still more visible for FSC equal to three.

The failure on one cell observed for ageing times around 450 h has appeared quite suddenly. By observing the graphs of Fig. 7, the difficulty encountered to operate the FC at FSA = 1.5 during the first 450 h of the ageing test can be observed. The polarisation curve records were generally interrupted for load currents near 50 A. This FC behaviour can be considered as a premonitory pattern for the encountered problem. Notice that the deterioration rate of the "mean single cell" performances is globally not so strong, in particular if a comparison is done with the results obtained in the reference test. To this aim, Fig. 8 shows the example of the contour plots computed for FSA/FSC = 2/4 in the case of the reference test [14]. Eq. (6) has been used to display the surface response of the model related with this exper-

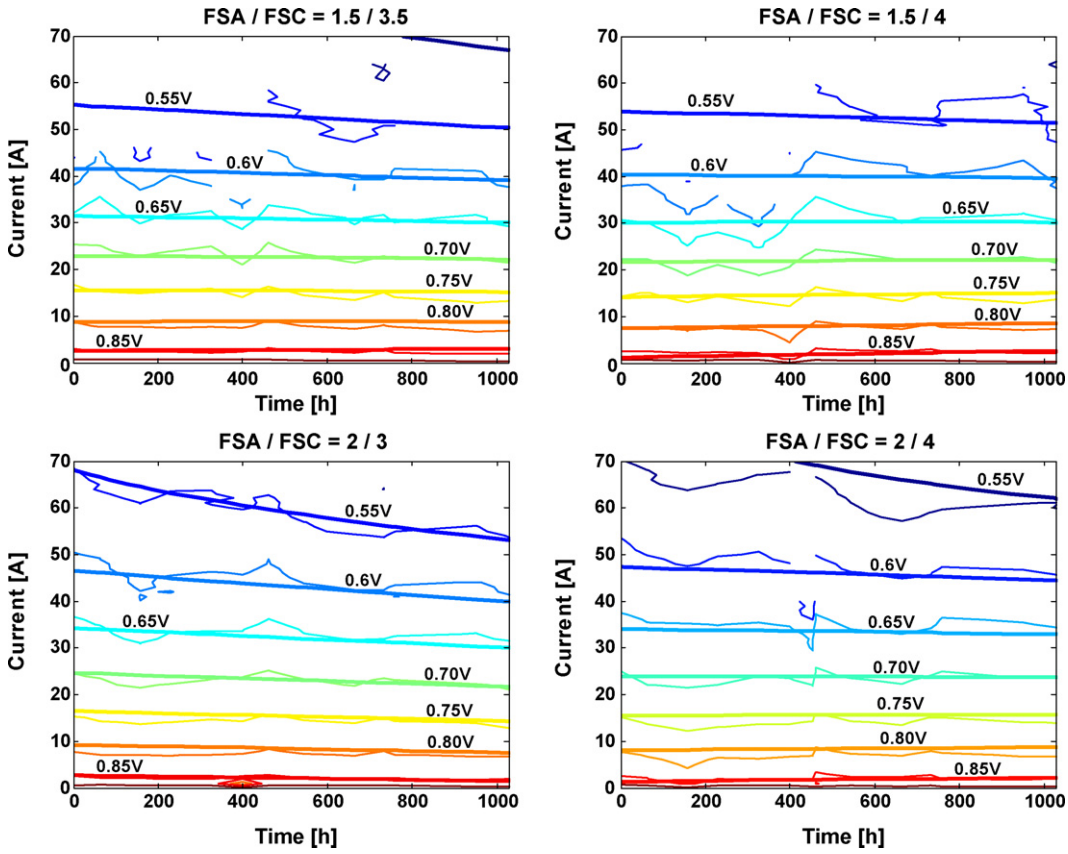

Fig. 7. Contour plots displayed for the experimental measurements (dotted lines) and for the full quadratic model (full lines) in the case of the low humidity test.

iment. Not that the order of the polynomial model is not high enough to reproduce the slight improvement of the performances at the beginning of the test ($0 < t < 100$ h). However the model is sufficient to fit the global trend over the 1000 h of operation.

$$U_{\text{mean cell RSM 1st ref test}} = 0.6037 - 0.2070 \times I - 0.0395 \times t + 0.0098 \times \text{FSC} + 0.1078 \times I^3 - 0.0204 \times t^2 - 0.0043 \times \text{FSC}^2 - 0.0221 \times I \times t + 0.0146 \times I \times \text{FSC} + 0.0211 \times t \times \text{FSC} + \varepsilon \quad (6)$$

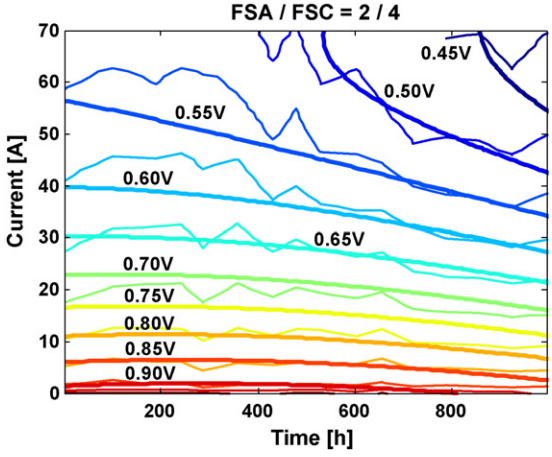

Fig. 8. Contour plots displayed for the experimental measurements (dotted lines) and for the full quadratic model (full lines) in the case of the reference test (FSA/FSC = 2/4).

Even though the models proposed in this study cannot be considered as physical models (indeed, they are rather statistical models), they can be helpful to clearly dissociate the respective impacts of the various physical parameters over the investigated response. For instance, the approach allows the dissociation of the cell voltage drop due to the ageing time from the voltage evolutions caused by the setting of different operating conditions (e.g. load current and air stoichiometry rate values).

4.2.3. *Optimisation of the operating conditions*

The optimisation goal is to define the hydrogen/air stoichiometry rates leading to the highest FC voltage in the time and current ranges explored. The programming problem satisfying the constraints $1.5 < \text{FSA} < 2$ and $3 < \text{FSC} < 5$ can be solved thanks to the *quadprog* Matlab$^{\text{TM}}$ function [30]. Fig. 9 shows the results of the optimisation. FSA equal to 2 leads to the highest stack performances for the complete experimental domain investigated, thus no graph related with this result is displayed. FSC equal to three allows obtaining the best performances only at the very beginning of the ageing test and for low current

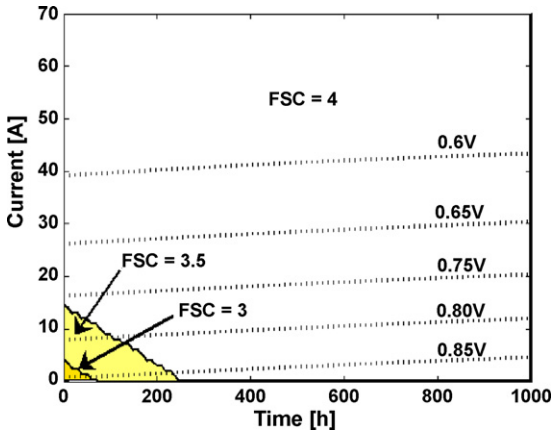

Fig. 9. Contour plot of the response surface for FSC leading to the highest performances and related optimal "mean cell" voltage.

values. Then, with time, FSC equal to 5 becomes necessary to reach the highest stack voltage. This result is quite similar with the one already obtained in the case of the reference test [14]. The need of a growing air supply can be explained by different factors. The increase of the crossover rate through the defective cell during the first 450 h of operation consumes some reactive gases, which thus cannot serve the electrochemical reaction and the delivery of high cell potentials. Therefore, some additional reactive gas flow quantities are requested in order to balance the leakage flow passing in the possible membrane pinholes. Besides, the gas flow value crossing the failed membrane can be governed by the total pressure gradient between the anode and cathode compartments, which is linked here with the FSA/FSC rates since there is no back-pressure control in the experiment. According to the sign of this pressure gap, more or less fuel or oxidant can pass through the failed membrane and affect the cell potential. Another probable explanation about the rising need of higher oxidant flows can concern the ageing of the GDLs. Some poorer gas diffusion properties can affect the water removal inside the cells, especially at cathode, and they can induce a higher demand of air-flow rates to enable good cell performances. Another concern is the reduction of the electrode active areas throughout the ageing time (caused by poorer catalyst layer properties).

4.3. Electrochemical impedance spectroscopy

The EIS test results of the durability experiment performed in low humidity conditions are employed to get a deeper understanding of the impact of ageing time over the FC voltage, by considering here some various FSC levels. The electrochemical impedance spectra are used to provide some additional physical interpretations and also to corroborate the observations already made from the static measurements. For this purpose, some RSM full factorial designs are used to analyse the endurance test and to establish some preliminary models for two important parameters related with the recorded EIS spectra, namely internal resistance and polarisation resistance. Obviously, the evolutions of these experimentally measured parameters could be directly plotted on various graphs as a function of ageing time and for the different investigated FSC rates. But one of the RSM strength is also to provide some concise graphs or maps that allow an overall picture and a better visualisation of the response trends according to the selected factors and test conditions.

4.3.1. Internal resistance

A full factorial design is first used to select the data that will enable the creation of two response surfaces: one for the stack composed of three cells and another one for the two-cell stack. The levels adopted for the factors are summarised in Table 2.

In a second step, two quadratic polynomial models are computed from the data grids generated. The related Eqs. (7) and (8) as well as their respective R^2 coefficients are given, on the one hand for the three-cell stack and on the other hand for the two-cell stack. Note that the model quality, which is not very high in this case, can be explained by the small range of the internal resistance variation.

$$\hat{R}_{\text{int}_{3\text{cells}}}\ (\text{m}\Omega) = 4.528 + 0.015 \times t + 0.168 \times \text{FSC} - 0.007 \times t^2 - 0.037 \times \text{FSC}^2 - 0.052 \times t \times \text{FSC} \quad (7)$$

$$\hat{R}_{\text{int}_{2\text{cells}}}\ (\text{m}\Omega) = 3.436 + 0.01 \times t + 0.107 \times \text{FSC} + 0.041 \times t^2 - 0.033 \times \text{FSC}^2 - 0.043 \times t \times E \quad (8)$$

For the three cell stack : $R^2 = 0.8613$,

for the two cell stack : $R^2 = 0.7911$

The two models proposed are then used to display some contour plots of the internal resistance in the ageing time–FSC plane (Fig. 10). The decrease of the cathode stoichiometry, from five to three, leads to a slight drop of the internal resistance. This is due to the fact that in the experimental domain explored, some higher air flows cause a drying of the membranes. Fig. 10 shows that the time factor has no large impact on the internal resistance

Table 2
Levels of the investigated factors for the study of the internal resistance

Factors	Levels			
	Minimum (−1)	Intermediate	Maximum (+1)	Number
t	0 h (three-cell stack) 460 h (two-cell stack)	Characterisation instants	398 h (three-cell stack) 952 h (two-cell stack)	6
FSC	3	4	5	3

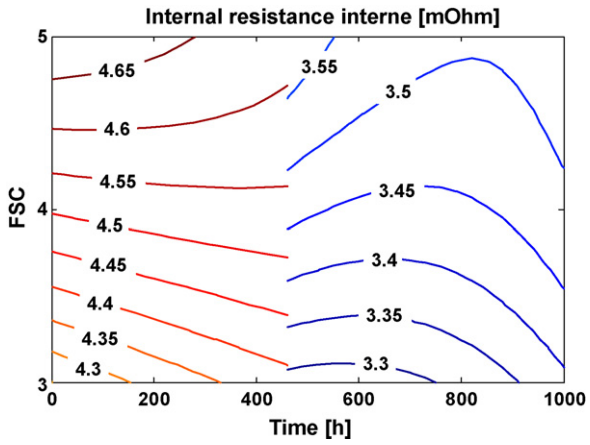

Fig. 10. Contour plots displayed for the internal resistance measured at 55 °C (during the characterisations).

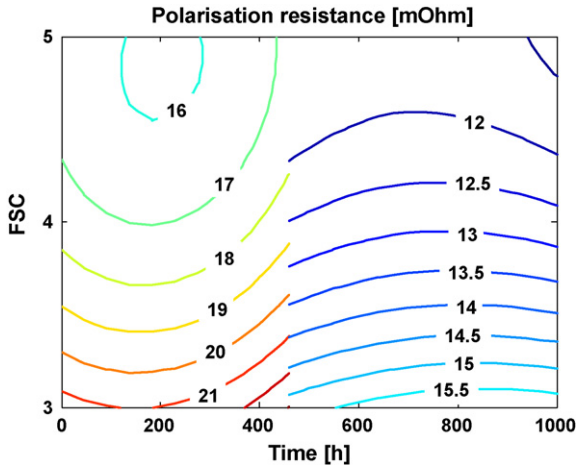

Fig. 11. Contour plots displayed for the polarisation resistance (stack temperature of 55 °C).

variation, which remains restrained. It is highly probable that the membranes were affected by the stack operation at low humidity conditions and thus could deteriorate more rapidly, leading finally to the formation of holes in one of the cell membranes. According to [31], the membrane thinning and cracks or holes can be caused by different physical phenomena: for instance, the dissolution of the polymer followed by peroxide attack, the loss of sulfonic acid groups. Here, the evolution of the internal resistance versus ageing time does not give any significant proof of the membrane material degradation. As stated in Section 3.1, the abnormal behaviour of the cell OCV is rather to be considered in order to detect any larger crossover rate of the reactive gases through the membrane pinholes. Possibly, the decomposition of the membrane could also be observed by detecting some fluoride ion releases in the FC exhaust waters. Note that by considering Fig. 10, it is also possible that the membrane degradation does not negatively affect the cell performances, at least during a first ageing time period, since the membrane thinning might also reduce the membrane resistance and thus lead to lower performance losses.

4.3.2. Polarisation resistance

The same approach is used to propose some models and display some response surfaces in the case of the polarisation resistance study. So, a full factorial design is first generated considering the factors levels of Table 2. Then, two quadratic models are calculated for the three-cell and two-cell stacks. The response surfaces related with the polarisation resistance evolution are presented in the plane ageing time–FSC plane (Fig. 11). Finally, some observations can be made from the graph.

The consequence of a FSC increase is a drop down of the polarisation resistance, i.e. higher FC electrical performances. During the 180 first hours of the test and for a given FSC value, the response surface shows a decrease of the polarisation resistance (hence an improvement of the stack voltage). This initial time period may be compared with the phases of "running in" that are sometimes encountered with engines. Note that the phenomenon was also observed in the case of the first ageing reference test (Fig. 3). The improvement of the stack performances at the test beginning can be explained by various factors: a progressive better hydration of the membranes (especially at the anode since there is no humidification of the fuel upstream of the stack) leading to a higher electrolyte conductivity (Fig. 10), some better interface contacts between the different MEA components, possibly also by a gradual elimination of solvent traces and other residual constituents linked with the MEA manufacturing process. After that, between the 200th and 460th hour, and still for a given FSC value, an increase of the polarisation resistance (corresponding to a degradation of the FC voltage) occurs. It can be attributed to the higher crossover rate in the defective cell. The 540 next hours, which correspond to the operation with the two-cell stack, give rise to a stabilisation of the FC performances.

$$\hat{R}_{\mathrm{pola_{3cells}}}\ (\mathrm{m}\Omega) = 17.014 + 0.522 \times t - 2.611 \times \mathrm{FSC} + 1.125 \times t^2 + 1.487 \times \mathrm{FSC}^2 - 0.275 \times t \times \mathrm{FSC} \quad (9)$$

$$\hat{R}_{\mathrm{pola_{2cells}}}\ (\mathrm{m}\Omega) = 12.889 + 0.091 \times t - 2.027 \times \mathrm{FSC} - 0.290 \times t^2 + 0.892 \times \mathrm{FSC}^2 - 0.190 \times t \times \mathrm{FSC} \quad (10)$$

For the three cell stack : $R^2 = 0.9779$,

for the two cell stack : $R^2 = 0.9605$

When increasing the cathode stoichiometry rate for a given ageing time, a higher polarisation resistance can be observed while a rather lower internal resistance is detected. In this case, the loss of FC global performances can rather be attributed to difficult charge transfer and species diffusion since the polarisation resistance corresponds to the global sum of the various resistances (internal resistance, transfer resistance, etc.) linked with the different physical phenomena involved in the stack. Besides, the effects of mass transfer limitations could already

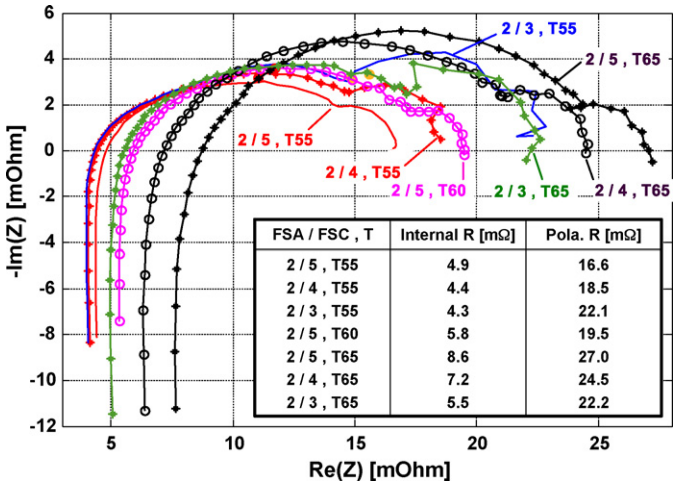

Fig. 12. Set of impedance spectra recorded prior the durability test (EIS measurements performed for different FSA/FSC rates and stack temperatures, with dry hydrogen and humidified air—dew point temperature of 25 °C).

be observed from the polarisation curves at high current density. These statements can be made for the entire duration of the ageing test. However, the FSC impact over the evolution of the internal and polarisation resistances would be different for a stack temperature equal to 65 °C and identical gas humidification conditions (i.e. FC fed with dry hydrogen and air with a dew point temperature of 25 °C). A few electrochemical impedance spectra were recorded with these operating parameters before the beginning of the ageing test, with the aim to investigate the impact of temperature over the FC performances. Some of these records are depicted in Fig. 12 and it can be observed that both internal and polarisation resistance values increase significantly at 65 °C for a higher FSC rate. The increase of the internal resistance can be explained by the water removal and the drying out in the membranes and in any ionomer present in the catalyst layers. The rise of the polarisation is obviously due to the higher internal resistance, but probably also to a higher charge transfer resistance as the diameter of the high-medium frequency arc appears as larger (electrode dehydration).

5. Conclusion

The impact of low humidity conditions on the FC durability and reliability has been investigated by operating a three-cell stack during 1000 h and by characterising it regularly throughout ageing time, using both polarisation curve and EIS measurements performed for different gas flow rates. Some design of experiment techniques and in particular the response surface methodology have been employed to analyse the results of the considered ageing test. The DoE methodology proved to be really suitable to analyse the degradation of FC operated in different conditions, in particular by providing some graphic tools that enable fine overall pictures of the investigated phenomena. The approach would be quite difficult to apply by considering many levels of parameters related with various ageing conditions since the total duration of the complete durability test set would lead in this case to huge experiment durations. However, the methodology seems to be rather appropriate to explore different operating conditions during the stack characterisation sequences within an ageing test (as in the proposed work). These characterisations can be used especially to highlight and to better understand the degradation phenomena.

In this work, some numerical models have been proposed from the static current—voltage records to study the impact of stoichiometric rates over the performance deterioration. Although one of the three cells failed around the 450th hour of stack operation, a quite weak degradation rate was observed for the "mean single cell" performances. Some numerical/statistical models have been computed from the EIS data. The monitoring of the membrane conductivity through EIS measurements was really suitable to obtain some information related with the electrolyte hydration state. It is quite obvious that a FC operation with a higher internal resistance will probably reduce the stack lifetime expectancy and increase the probability of failing cell occurrence. Moreover, a simple survey of the internal resistance value seems to be inefficient to predict the coming next cell failures due to low humidity conditions. The ability to operate the stack with lower anode stoichiometry rate or the OCV monitoring should rather be used as a diagnosis tools allowing the detection of hydrogen crossover rate through the electrolytes. However, it is still very difficult to give some accurate reasons that could explain why one cell failed and not the two other ones. One can suggest for instance that a local imperfection, formed during the MEA manufacturing, or a minor damage, caused during the beginning of the FC testing, such as a crack, could act as a stress concentrating point. Some more fundamental understanding of physical ageing mechanisms through post-mortem analyses by chemists or electrochemists could certainly help us in this way [32,33]. From an experimental point of view, better test designs combined with the use of multiple characterisation methods in parallel (e.g. crossover and cyclic voltammetry measurements) are required to ensure that the maximum amount of information is obtained from the ageing experiments.

The final results of the durability program should be used to propose some technological solutions for future FC generators as well as test methodologies, which could provide a convenient help to define the tradeoffs at the system level leading to extended lifetimes.

Acknowledgment

Financial support by the French Government under contract 01Y0044-02 is gratefully acknowledged.

References

[1] S.D. Knights, K.M. Colbow, J. St-Pierre, D.P. Wilkinson, J. Power Sources 127 (March (1–2)) (2004) 127–134.
[2] A. Collier, H. Wang, X.Z. Yuan, J. Zhang, D.P. Wilkinson, Int. J. Hydrogen Energy 31 (October (13)) (2006) 1838–1854.
[3] A. Taniguchi, T. Akita, K. Yasuda, Y. Miyazaki, J. Power Sources 130 (2004) 42–49.
[4] Z. Liu, L. Yang, Z. Mao, W. Zhuge, Y. Zhang, L. Wang, J. Power Sources 157 (June (1)) (2006) 166–176.
[5] H. Tang, S. Peikang, S.P. Jiang, F. Wang, M. Pan, J. Power Sources 170 (June (1)) (2007) 85–92.

[6] A. Husar, M. Serra, C. Kunusch, J. Power Sources 169 (June (1)) (2007) 85–91.
[7] B. Wahdame, D. Candusso, X. François, F. Harel, A. De Bernardinis, J.-M. Kauffmann, G. Coquery, Study of a 5 kW PEMFC Using Experimental Design and Statistical Analysis Techniques, Fuel Cells from Fundamentals to Systems, vol. 7, Wiley–VCH, 2007, pp. 47–62.
[8] S. Yoshioka, A. Yoshimura, H. Fukumoto, O. Hiroi, H. Yoshiyasu, J. Power Sources 144 (June (1)) (2005) 146–151.
[9] F.N. Büchi, S. Srinivasan, J. Electrochem. Soc. Fundam. Aspects 144 (August (8)) (1997) 2767–2772.
[10] J.R. Atkins, S.C. Savett, S.E. Creager, J. Power Sources 128 (April (2)) (2004) 201–207.
[11] Z. Qi, A. Kaufman, J. Power Sources 109 (July (2)) (2002) 469–476.
[12] F. Harel, X. François, D. Candusso, D. Hissel, M.-C. Péra, J.-M. Kauffmann, Proceedings of the France–Deutschland Fuel Cell Conference 2004 on Fuel Cells: Materials, Engineering, Systems and Applications (FDFC 2004), Belfort, France, 29 November–2 December, 2004, ISBN 2914279-16-7, pp. 365–370.
[13] F. Harel, X. François, D. Candusso, M.-C. Péra, D. Hissel, J.-M. Kauffmann, PEMFC Durability Test Under Specific Dynamical Current Solicitation Linked to Vehicle Road Cycle, Fuel Cells from Fundamentals to Systems, vol. 7, Wiley–VCH, 2007, pp. 142–152.
[14] B. Wahdame, D. Candusso, X. François, F. Harel, M.-C. Péra, D. Hissel, J.-M. Kauffmann, Proceedings of the IEEE International Symposium on Industrial Electronics (ISIE 2006), vol. 3, Montréal, Canada, July 9–13, 2006, ISBN 1-4244-0497-5, pp. 2007–2012.
[15] B. Wahdame, D. Candusso, X. François, F. Harel, M.-C. Péra, D. Hissel, J.-M. Kauffmann, Proceedings of the IEEE IECON'06 (Industrial Electronics Conference), Paris, November 7–10, 2006, pp. 4337–4342.
[16] D. Hissel, M.C. Péra, D. Candusso, F. Harel, S. Bégot, in: X.-W. Zhang (Ed.), Advances in Fuel Cells: Research Signpost, North Carolina State University, 2005, ISBN 81-308-0026-8.
[17] F. Harel, X. François, S. Jemeï, S. Moratin, Conception et réalisation d'un banc d'essai pour piles à combustibles à membrane de faibles puissances, INRETS Report, LTE no. 0310, May 2003, Belfort, France.
[18] R. Glises, D. Hissel, F. Harel, M.C. Péra, J. Power Sources 150 (October (4)) (2005) 78–85.
[19] G.H. Guvelioglu, H.G. Stenger, J. Power Sources 163 (January (2)) (2007) 882–891.
[20] FUERO Specification of Tests Procedures for PEM Fuel Cell Stacks, Draft version 3, Prepared by the FUERO Consortium with Volvo as principal author, March 2003.
[21] Final FCTESTNET Meeting Presentations Estoril, 2 and 3 February 2006, http://www.jrc.nl/fctestnet.
[22] G. Taguchi, Introduction to Quality Engineering, Asian Productivity Organization, 1986, Distributed by American Supplier Institute Inc., Dearborn, MI.
[23] Sleem-ur-Rahman, M.A. Al-Saleh, A.S. Al-Zakri, J. Power Sources 72 (March (1)) (1998) 71–76.
[24] L. Ion-Boussier, S. Benhabib, A. Mièze, F. Duclaud, Proceedings of the Electric Vehicle Symposium 21 (EVS21), Monaco, April 2–6, 2005.
[25] J.R. Miller, D.A. Evans, Proceedings of the IEEE 35th International Power Sources Symposium, June 22–25, 1992, pp. 302–305.
[26] R.C. Dante, J.L. Escamilla, V. Madrigal, T. Theuss, J. de Dios Calderon, O. Solorza, R. Rivera, Int. J. Hydrogen Energy 28 (March (3)) (2002) 343–348.
[27] B. Wahdame, D. Candusso, J.M. Kauffmann, J. Power Sources 156 (May (1)) (2006) 92–99.
[28] M. Ordonez, M. Tariq Iqbal, J.E. Quaicoe, L.M. Lye, Canadian Conference on Electrical and Computer Engineering, 2006, pp. 1120–1124.
[29] G.E.P. Box, W.G. Hunter, J.S. Hunter, Statistics for Experimenters: An Introduction to Design, Data Analysis and Model Building, John Wiley & Sons, 1978, ISBN 0-471-09315-7.
[30] Statistics Toolbox, Optimization Toolbox For Use with MATLAB®, The MathWorks, Inc., http://www.mathworks.com.
[31] D.P. Wilkinson, J. St-Pierre, Handbook of Fuel Cells—Fundamentals, Technology and Applications, vol. 3, John Wiley & Sons, 2003, pp. 611–626, Chapter 47.
[32] M.K. Debe, A.K. Schmoeckel, G.D. Vernstrom, R. Atanasoski, J. Power Sources 161 (October (2)) (2006) 1002–1011.
[33] R.L. Borup, J.R. Davey, F.H. Garzon, D.L. Wood, M.A. Inbody, J. Power Sources 163 (December (1)) (2006) 76–81.